Supplementary Material

F, P double-doped Fe_3O_4 with abundant defect sites for efficient hydrogen evolution at high current density

Xin-Yu Zhang [a], Feng-Ting Li [b], Ruo-Yao Fan [a], Jie Zhao [a], Bin Dong [*a],

Fu-Li Wang [a], Hai-Jun Liu [a], Jian-Feng Yu [a], Chen-Guang Liu [a], Yong-Ming Chai [*a]

a State Key Laboratory of Heavy Oil Processing, College of Science, China University of Petroleum (East China), Qingdao 266580, PR China

b College of Materials Science and Engineering, China University of Petroleum (East China), Qingdao 266580, PR China

∗ Corresponding author. Email: dongbin@upc.edu.cn (B. Dong), ymchai@upc.edu.cn (Y. M. Chai)

Tel: +86-532-86981156, Fax: +86-532-86981156

Calculation of electrochemically active surface areas (ECSA)

The value of ECSA can be obtained by previously reported equations in the following:

$ECSA=C_{dl}/Cs$

C_{dl}: double layer capacitance of samples tested in 1.0 M KOH (mF cm^{-2});

C_s: specific capacitance. The value of C_s is 0.04 mF cm^{-2} in 1.0 M KOH;

Fig. S1

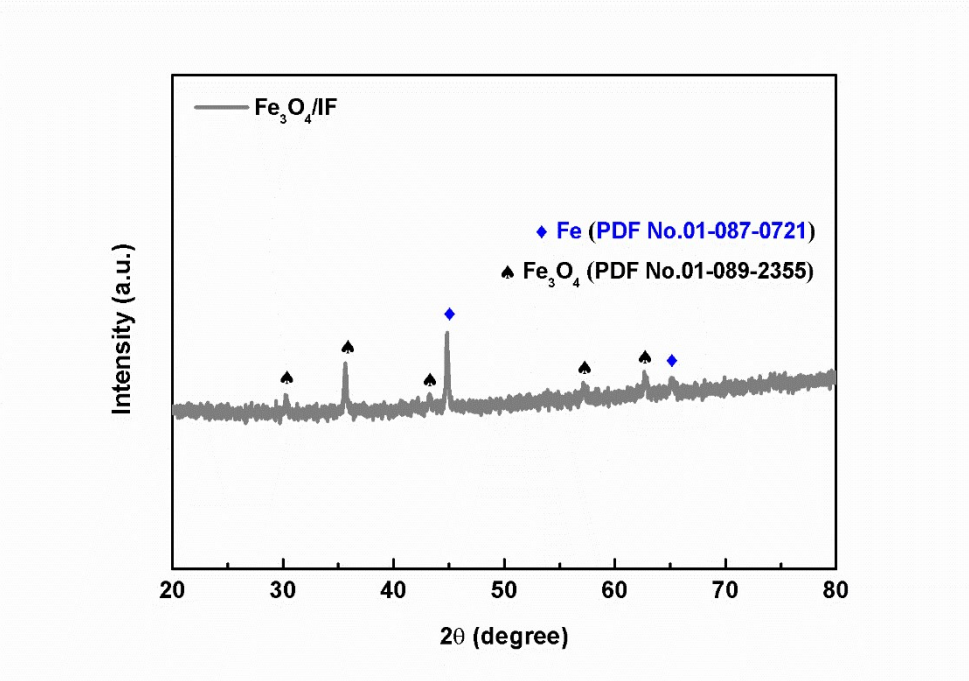

Fig. S1 XRD pattern of Fe_3O_4 supported on iron foam (Fe_3O_4/IF).

Fig. S2

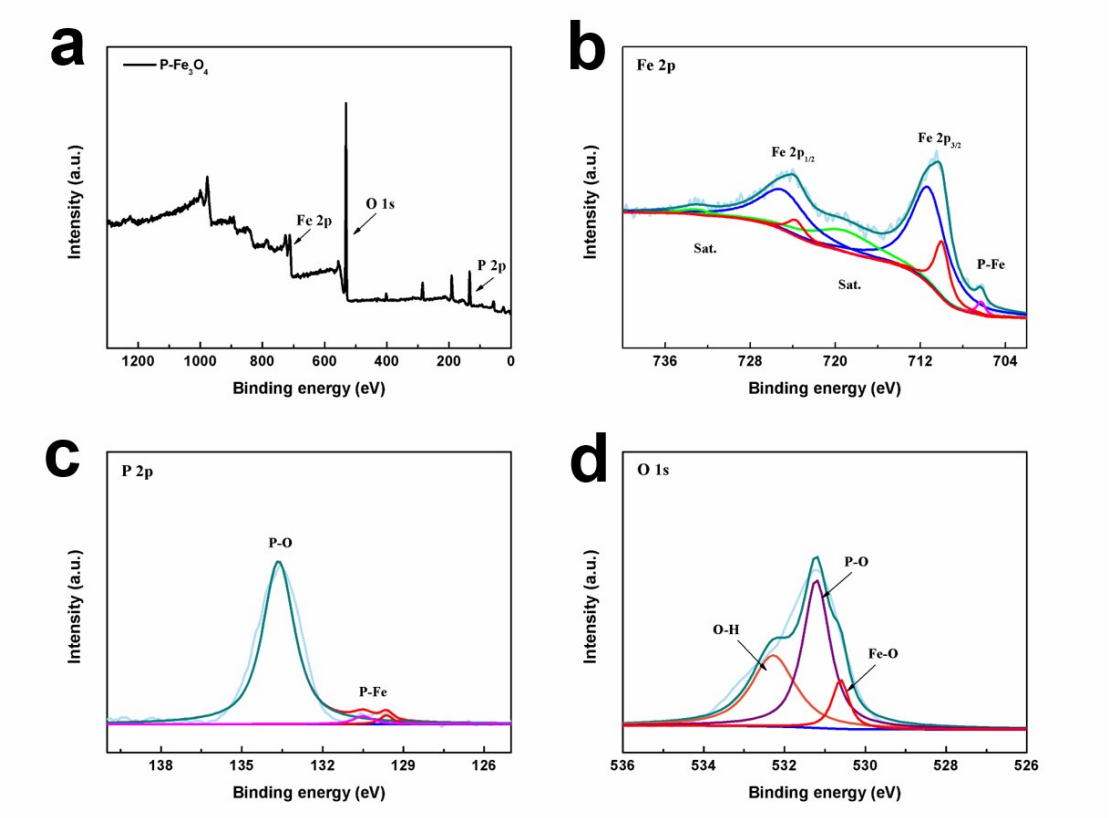

Fig. S2 XPS spectrum of (a) survey, (b) Fe 2p, (c) P 2p and (d) O 1s in P-Fe_3O_4/IF.

Fig. S3

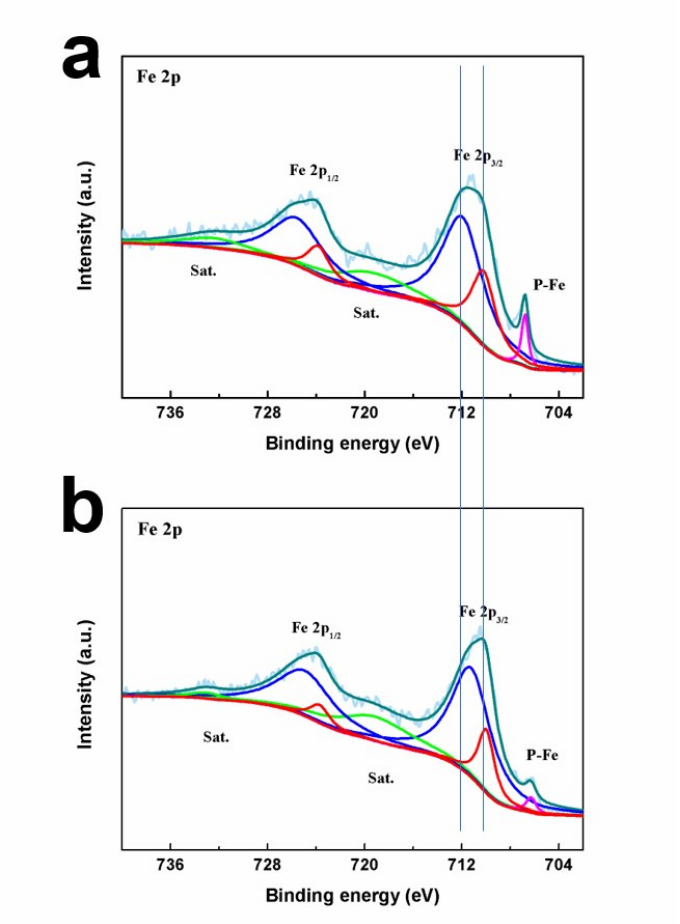

Fig. S3 The comparison of elements Fe in F, P-Fe_3O_4/IF (a) and P-Fe_3O_4/IF (b), respectively.

Fig. S4

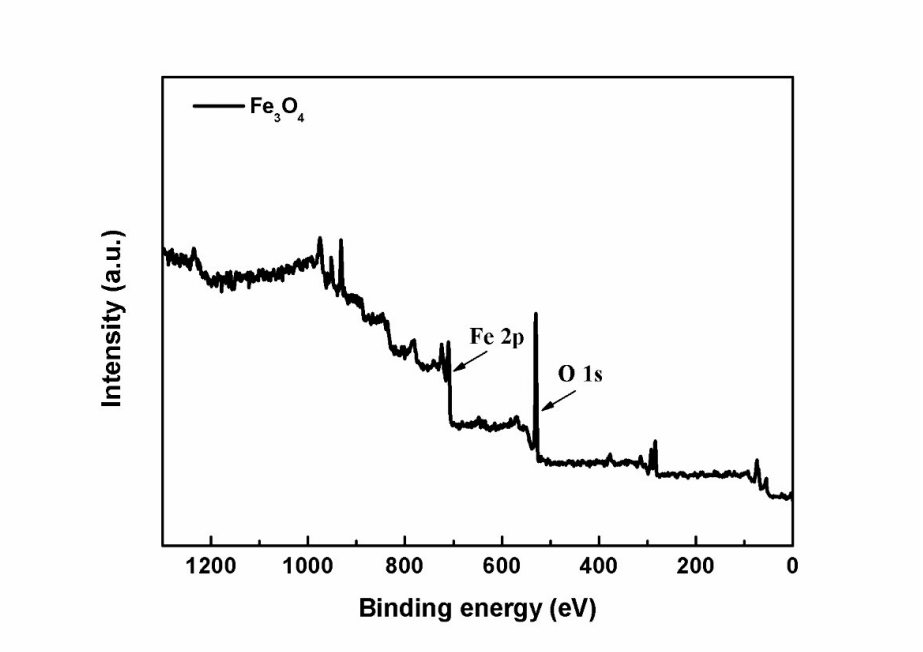

Fig. S4 XPS survey of Fe_3O_4 supported on iron foam (Fe_3O_4/IF).

Fig. S5

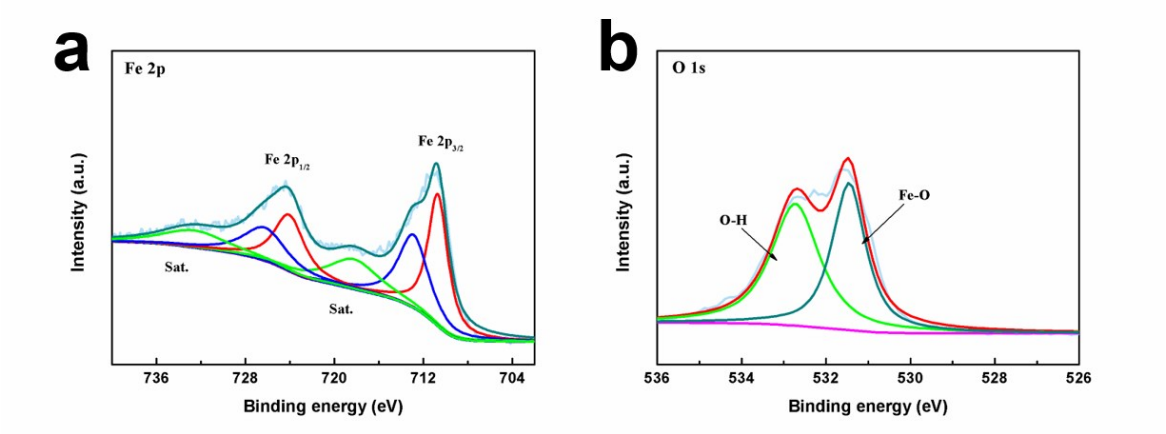

Fig. S5 XPS spectrum of (a) Fe 2p and (b) O 1s in Fe_3O_4/IF.

Fig. S6

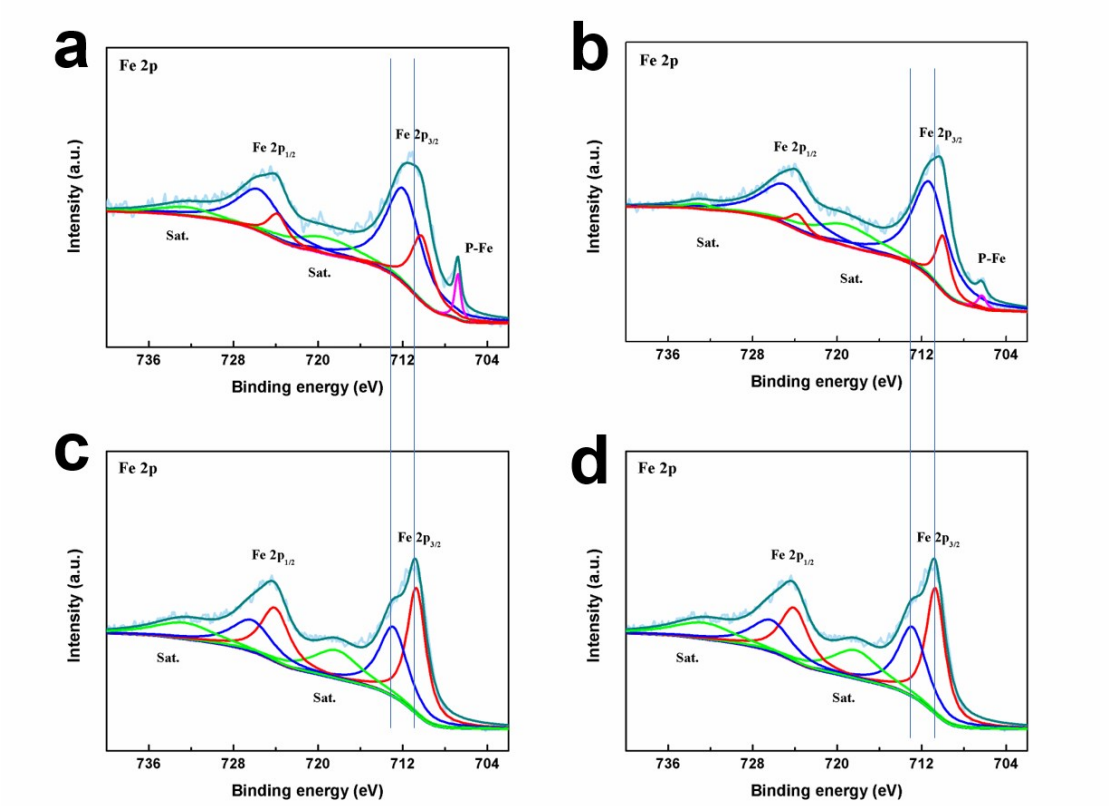

Fig. S6 The comparison of Fe in (a) F, P-Fe_3O_4/IF (b) P-Fe_3O_4/IF and (c-d) Fe_3O_4/IF, respectively.

Fig. S7

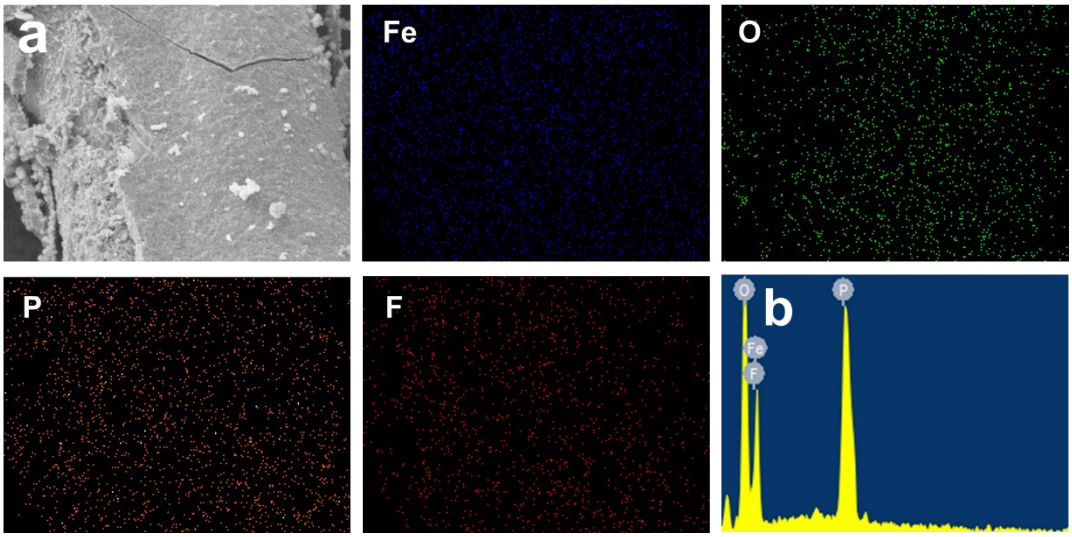

Fig. S7 SEM mapping of F, P-Fe_3O_4/IF.

Fig. S8

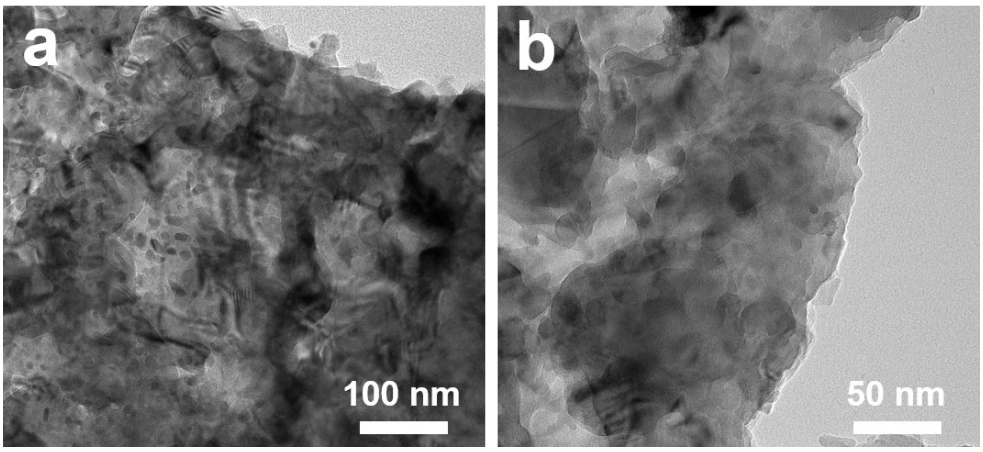

Fig. S8 TEM images of Fe_3O_4/IF.

Fig. S9

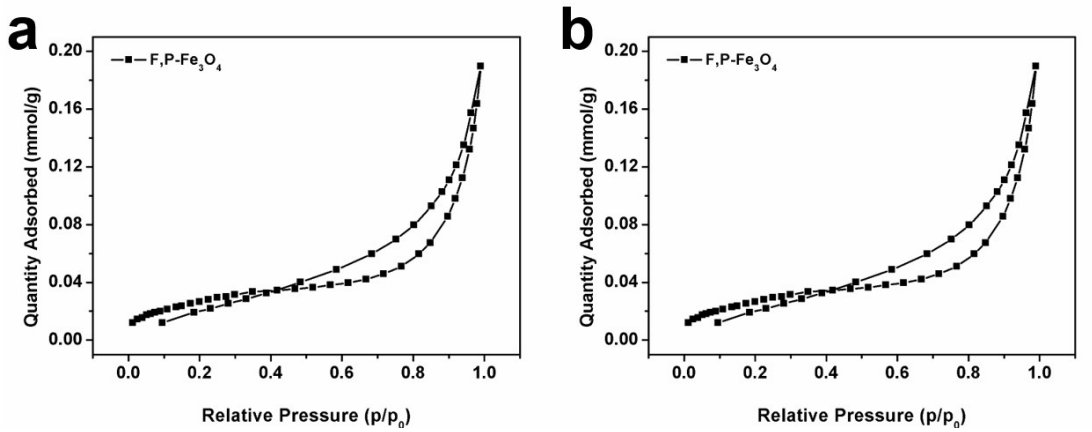

Fig. S9 The N_2 adsorption isotherms of F, P-Fe_3O_4 and Fe_3O_4.

Fig. S10

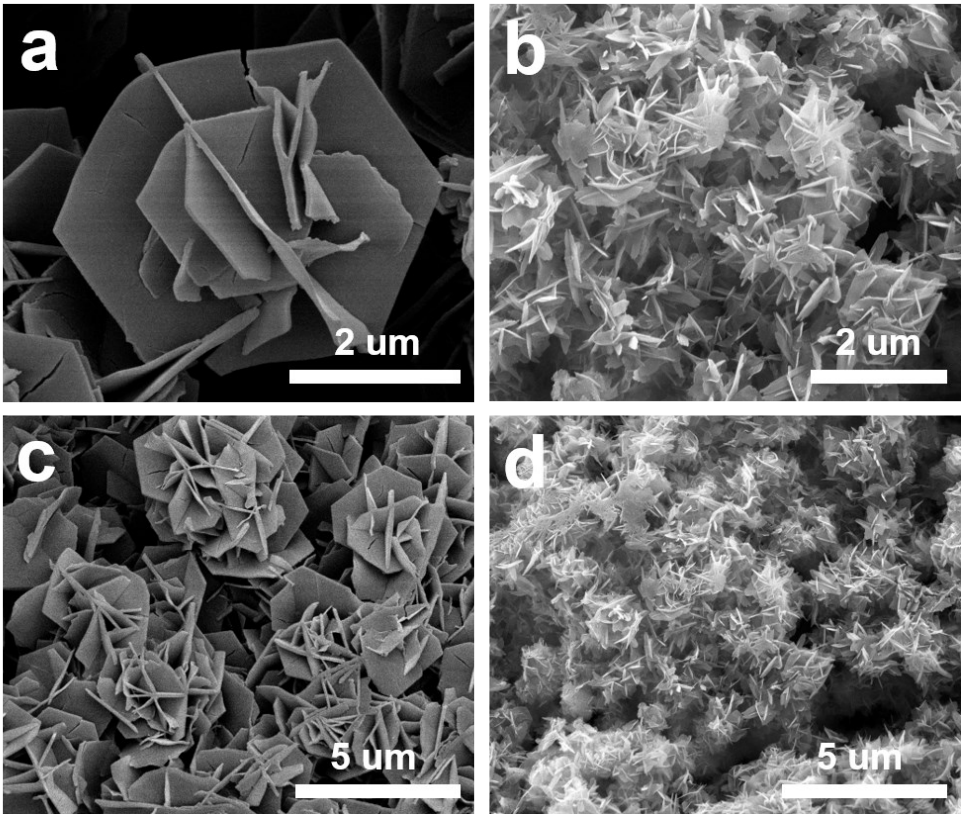

Fig. S10 SEM images of (a, c) FeOOH/IF and (b, d) FeO/IF.

Fig. S11

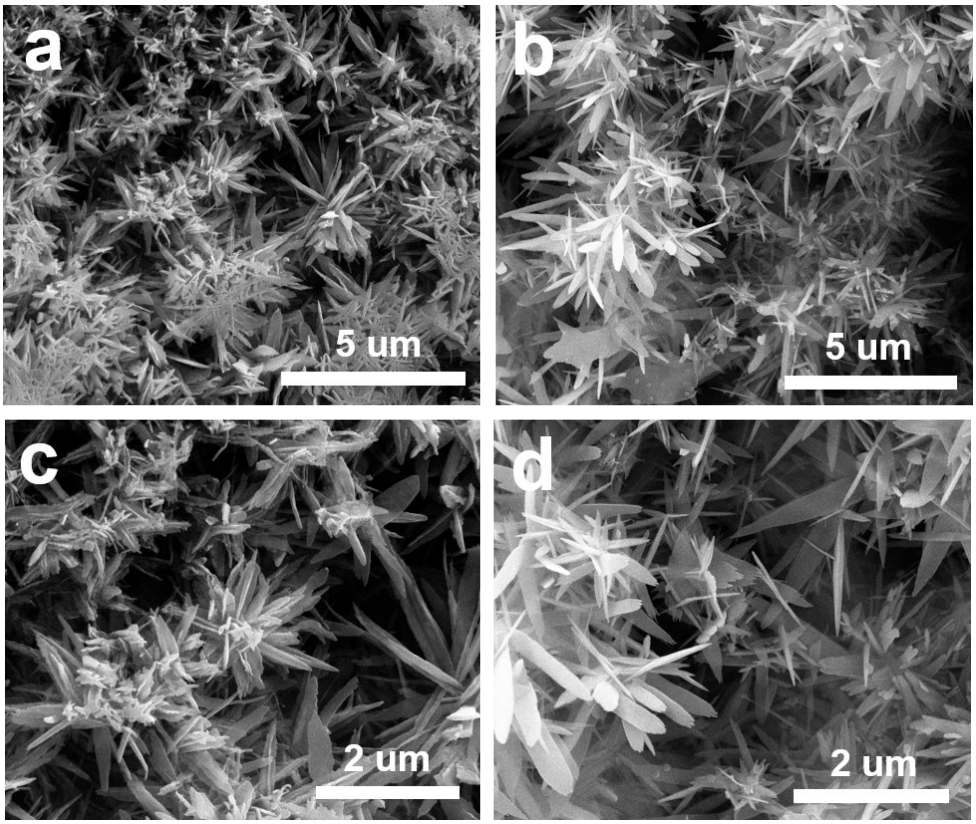

Fig. S11 SEM images of (a, c) P-Fe_3O_4/IF and (b, d) Fe_3O_4/IF.

Fig. S12

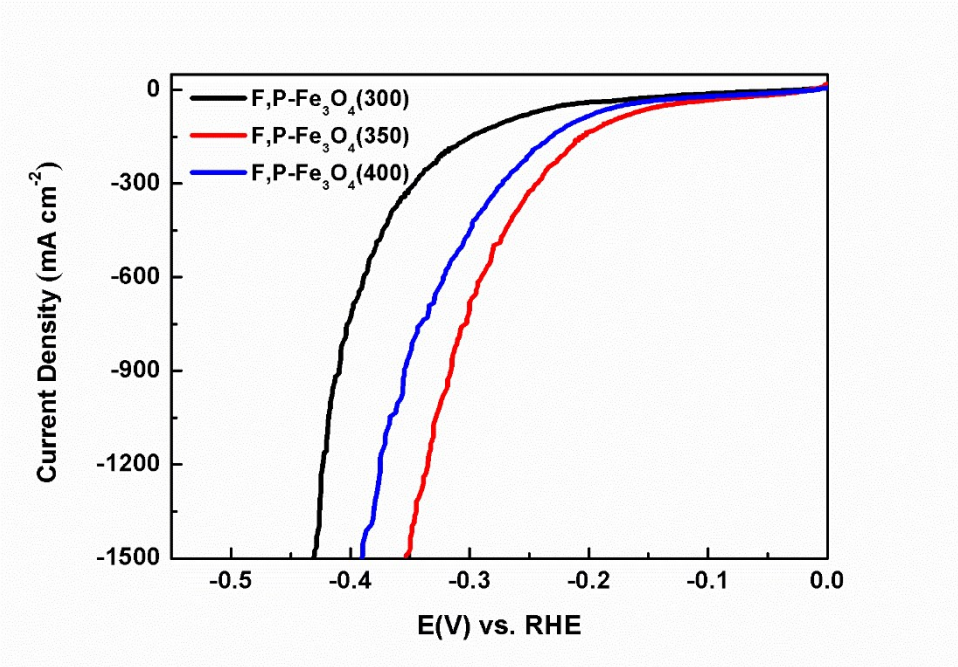

Fig. S12 HER polarization curves of F, P-Fe_3O_4/IF at different temperature.

Fig. S13

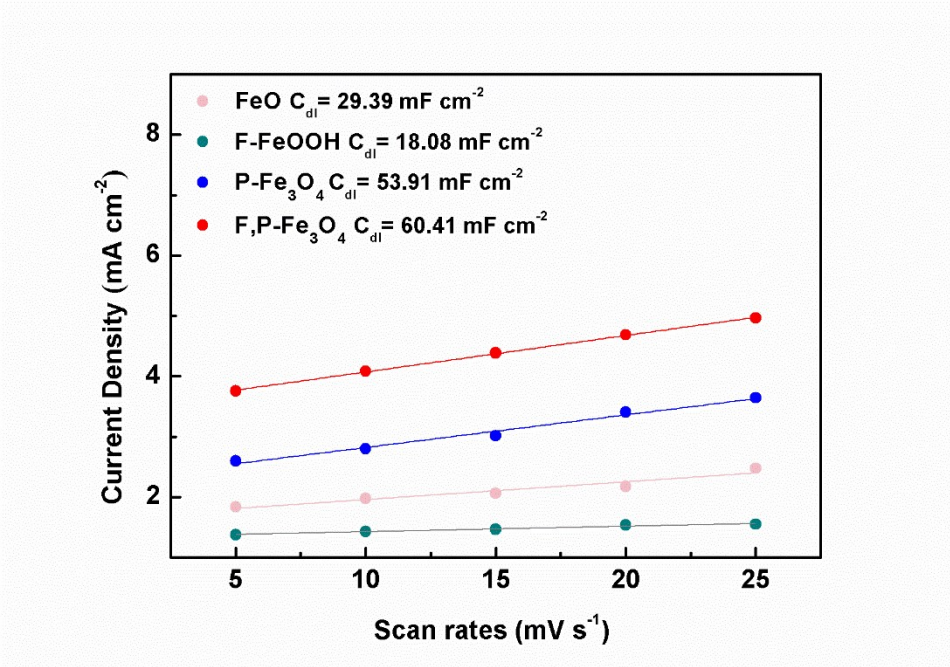

Fig. S13 The C_{dl} values of FeO, F-FeOOH, P-Fe_3O_4 and F, P-Fe_3O_4.

Fig. S14

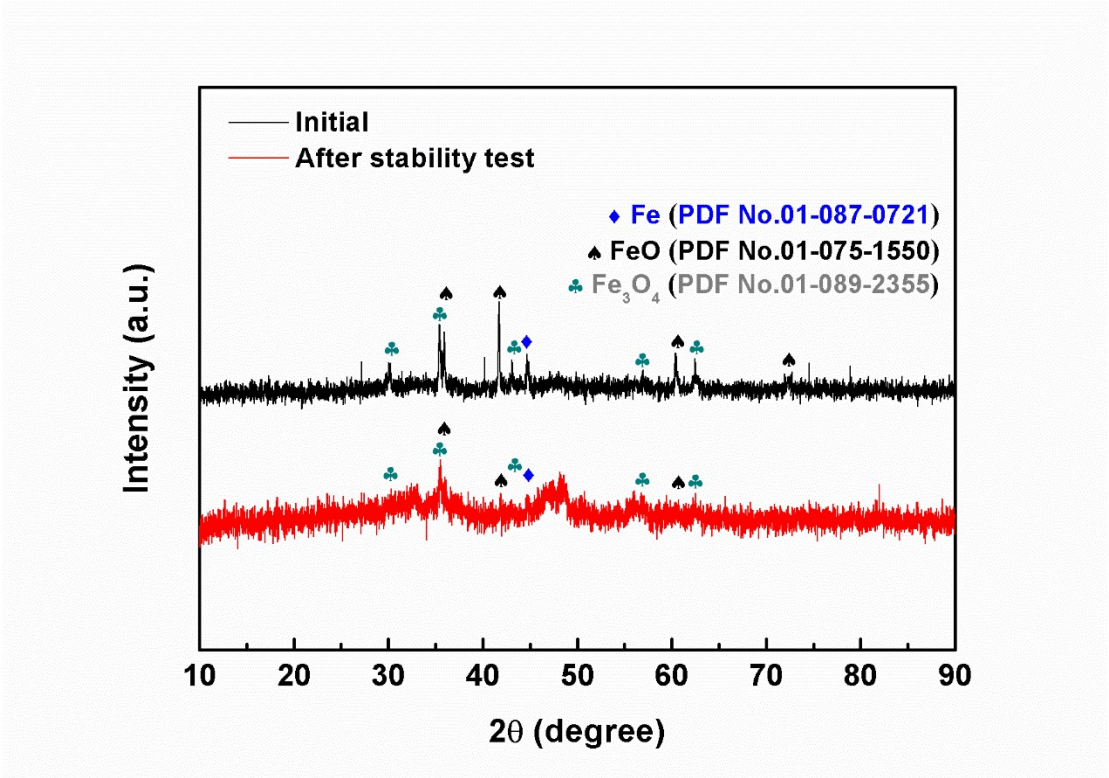

Fig. S14 XRD pattern of F, P-Fe_3O_4 after stability test.

Fig. S15

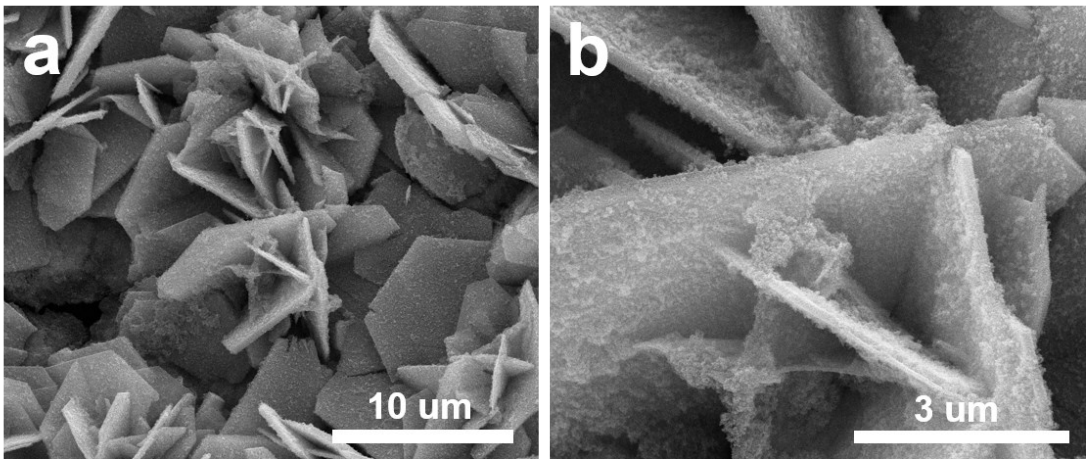

Fig. S15 SEM images after stability test for F, P-Fe_3O_4 at different scales.

Fig. S16

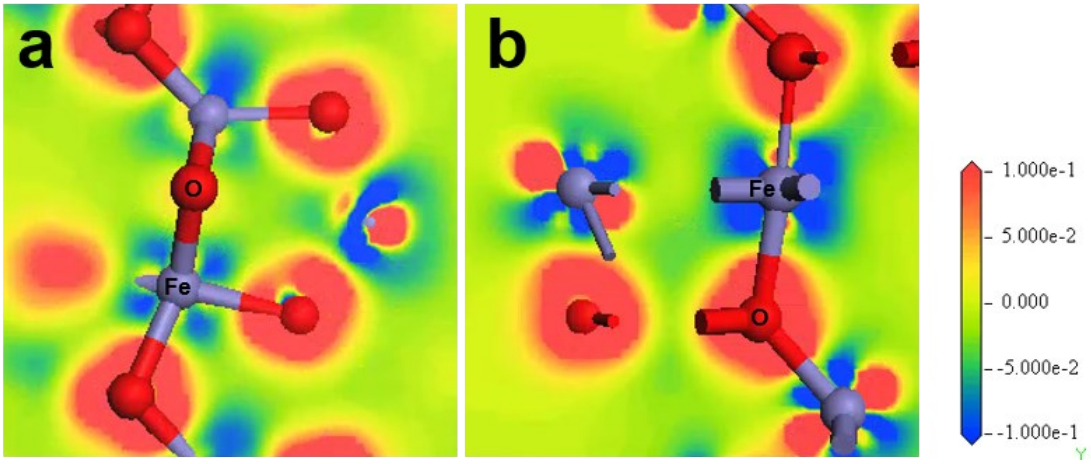

Fig. S16 Charge densities difference of Fe_3O_4 and F, P-Fe_3O_4.

Table S1

Table S1. The EDX data of P, F-Fe_3O_4.

Elements	Weight %	Atom %
Fe K	64.02	36.97
O K	25.07	50.54
P K	9.21	9.59
F K	1.71	2.90

Table S2

Table S2. Porosity condition of the F, P-Fe_3O_4 and Fe_3O_4. Where $S_{BET}/m^2/g$ is calculated by applying the BET equation using the linear part of the adsorption isotherm. $S_{micro}/m^2/g$ is calculated by t-plot method. $S_{meso}/m^2/g$ is calculated by BJH adsorption model.

Samples	**$S_{BET}/m^2/g$**	**$S_{micro}/m^2/g$**	**$S_{meso}/m^2/g$**
F,P-Fe_3O_4	2.36	1.31	1.81
Fe_3O_4	1.68	0.79	1.589

Table S3

Table S3. Comparison of HER performance of F, P-Fe_3O_4/IF with other electrocatalysts at 500 mA cm^{-2}.

Electrocatalyst	Electrolyte	Overpotential (mV)	Reference
F, P-Fe_3O_4/IF	1 M KOH	278	This work
NiO_x/Ni_3S_2	1 M KOH	307	[1]
$Ni_{11}(HPO_3)_8(OH)_6$	1 M KOH	385	[2]
Np-NiMn	1 M KOH	370	[3]
A-NiCo LDH/NF	1 M KOH	286	[4]
Sn-Ni_3S_2/NF	1 M KOH	356	[5]
IrNi/NF	1 M KOH	281	[6]
Fe_3O_4/IF	1 M KOH	348	[7]
Ni-MoO_2-450 NWs/CC	1 M KOH	320	[8]
MoS_2/Ni_3S_2/NF	1 M KOH	320	[9]
Pt/C/NF	1 M KOH	281	[10]

Table. S4

Table S4. The calculated values of ECSA of all samples.

Samples	**C_{dl} (mF cm^{-2})**	**Cs (mF cm^{-2} per cm^2)**	**ECSA(cm^{-2})**
FeO	29.39	0.04	734.57
F-FeOOH	18.08	0.04	452.00
P-Fe_3O_4	53.91	0.04	1347.75
F, P-Fe_3O_4	60.41	0.04	1510.25

Table S5

Table S5. The preparation cost of electrode per unit area of P, F-Fe_3O_4.

Materials	**Supplier**	**Used account (unit)**	**Cost (unit)**	**Cost (¥/m^2)**	**Sum cost**
Iron foam	Kunshan Tengerhui Electronic Technology Co. Ltd.	1 m^2	500 (¥/m^2)	500 ¥	848 ¥
Ammonium fluoride	Sinopharm Chemical Reagent Co. Ltd.	500 g	88 (¥/500g)	88 ¥	
Sodium hypophosphite	Sinopharm Chemical Reagent Co. Ltd.	2500 g	52 (¥/500g)	260 ¥	

References

[1] P.L. Zhai, Y.X. Zhang, Y.Z. Wu, J.F. Gao, B. Zhang, S.Y. Cao, Y.T. Zhang, Z.W. Li, L.C. Sun, J.G. Hou, Engineering active sites on hierarchical transition bimetal oxides/sulfides heterostructure array enabling robust overall water splitting, Nat. Commun. 5462 (2020) 11-23.

[2] P.W. Menezes, C. Panda, S. Loos, F. Bruns, C. Walter, A.M. Schwarze, X.H. Deng, H. Dau, M. Driess, A structurally versatile nickel phosphite acting as a robust bifunctional electrocatalyst for overall water splitting, Energy Environ. Sci. 11 (2018) 1287-1298.

[3] H. Liu, C. Xi, J.H. Xin, G.L. Zhang, S.F. Zhang, Z.J. Zhang, Q. Huang, J.X. Li, H. Liu, J.L. Kang, Free-standing nanoporous NiMnFeMo alloy: An efficient non-precious metal electrocatalyst for water splitting, Chemical Engineering Journal 404 (2021) 126530

[4] H.Y. Yang, Z.L. Chen, P.F. Guo, B. Fei, R.B. Wu, B-doping-induced amorphization of LDH for large-current-density hydrogen evolution reaction, Applied Catalysis B: Environmental 261 (2020) 118240-118252.

[5] J. Jian, L. Yuan, H. Qi, X.J. Sun, L. Zhang, H. Li, H.M. Yuan, S.H. Feng, Sn-Ni_3S_2 ultrathin nanosheets as efficient bifunctional water-splitting catalysts with a large current density and low overpotential, ACS Appl. Mater. Inter. 10 (2018) 40568-40576.

[6] Y.M. Wang, G.F. Qian, Q.L. Xu, H. Zhang, F. Shen, L. Luo, S.B. Yin, Industrially promising IrNi-$FeNi_3$ hybrid nanosheets for overall water splitting catalysis at large current density, Applied Catalysis B: Environmental 286 (2021)

119881.

[7] J.Q. Zhang, X. Shang, H. Ren, J.Q. Chi, H. Fu, B. Dong, C.G. Liu, Y.M. Chai, Modulation of inverse spinel Fe_3O_4 by phosphorus doping as an industrially promising electrocatalyst for hydrogen evolution, Adv. Mater. 12 (2019) 1905107-1905117.

[8] B.W. Ren, D.Q. Li, Q.Y. Jin, H. Cui, C.X. Wang, Integrated 3D self-supported Ni decorated MoO_2 nanowires as highly efficient electrocatalysts for ultra-highly stable and large-current-density hydrogen evolution, J. Mater. Chem. A 5 (2017) 24453-24461.

[9] N. Zhang, J. Lei, J.P. Xie, H.Y. Huang, Y. Yu, MoS_2/Ni_3S_2 nanorod arrays well-aligned on Ni foam: A 3D hierarchical efficient bifunctional catalytic electrode for overall water splitting, RSC Adv. 7 (2017) 46286-46296.

[10] S. Xue, Z.B. Liu, C.C. Ma, H.M. Cheng, W.C. Ren, A highly active and durable electrocatalyst for large current density hydrogen evolution reaction, Science Bulletin 65 (2020) 123-130